Initial Results from a Search for Lunar Radio Emission from Interactions of $\geq 10^{19}$ eV Neutrinos and Cosmic Rays

P. W. Gorham, K. M. Liewer, and C. J. Naudet
Jet Propulsion Laboratory, 4800 Oak Grove Dr. Pasadena, CA, 91109, USA

Abstract

Using the NASA Goldstone 70m antenna DSS 14 both singly and in coincidence with the 34 m antenna DSS 13 (21.7 km to the southeast), we have acquired approximately 12 hrs of livetime in a search for predicted pulsed radio emission from extremely–high energy cascades induced by neutrinos or cosmic rays in the lunar regolith. In about 4 hrs of single antenna observations, we reduced our sensitivity to impulsive terrestrial interference to a negligible level by use of a veto afforded by the unique capability of DSS 14. In the dual–antenna observations, terrestrial interference is eliminated as a background. In both observing modes the thermal noise floor limits the sensitivity. We detected no events above statistical background. We report here initial limits based on these data which strongly constrain several predictions of the flux of EHE neutrinos.

1 Introduction

Production of extremely high energy (EHE) neutrinos is expected to play an important role in the radiative kinematics of a number of cosmologically significant phenomena. Active Galactic Nuclei (AGN) may be copious producers of such neutrinos via hadronic interactions of particles energized by Fermi acceleration mechanisms at the predicted accretion shock near the central black hole. Cosmic gamma-ray bursts are expected to produce both cosmic rays and neutrinos through rapid shock acceleration during the burst and its gamma-ray afterglow. EHE cosmic rays themselves interact with a $\sim$ 10 Mpc mean free path with cosmic background photons to produce other EHE neutrinos. More exotic mechanisms such as topological defects or cosmic strings will also lead to EHE neutrino production.

Earth-based observatories for EHE neutrinos can only achieve adequate sensitivity by instrumenting a huge target mass. Optical Cherenkov detectors such as AMANDA and the European initiatives will in the next few years begin approaching the necessary sensitivity to detect cosmic neutrinos in the 10^{12-15} eV range. However, the EHE ($\geq 10^{18}$) eV regime is a much more difficult problem, and none of the existing instruments appear to have capability to address it. The required volume of water or ice to detect the extremely low flux densities at $\geq 10^{18}$ eV is in range of hundreds of cubic km per year of operation.

One proposed approach to this is to use detectors in the radio regime, sensing at large distances the emission of coherent radio Cherenkov radiation from the excess charge that develops in a EHE particle cascade. This method was first suggested by Askaryan (1962, 1965), and elaborated on by Dagkesamanskii & Zheleznykh (1989), whose work motivated one prior EHE neutrino search looking for radio emission from cascades in the lunar regolith (Hankins, Ekers, & O'Sullivan 1996) which reported a null result in 10 hours of livetime.

1.1 Emission Mechanisms & LINAC Results.

Recent work on modelling of coherent Cherenkov radio emission mechanisms in ice (Zas, Halzen & Stanev 1992) has provided detailed simulations the emission of radio Cherenkov radiation for cascade energies up to $\sim 10^{16}$ eV. This initial work was later extended by Alvarez-Muñiz & Zas (1997, 1998) in energy up to 10^{20} eV, including corrections as the Landau–Pomeranchuk–Migdal (LPM) effect. Related work by Zas and Alvarez–Muñiz (1996) considered the effects of the lunar regolith density and surface geometry on the propagation of the pulsed emission.

The conclusions of all of these modelling efforts have only strengthened the conclusion that lunar cascades should produce measurable pulsed emission at cm wavelengths. In fact, the radio emission is expected to peak at $\sim 1-2$ GHz, and extend up to $\sim$ 10 GHz before loss of coherence begins to significantly attenuate the signal. Thus the emission is well-matched to the receiving capabilities of many radio telescopes in the 2–20 cm-wavelength region.

Figure 1 plots the expected RF spectrum (upper) and pulse shape (lower) from a 10^{20} eV lunar cascade as received at Earth, including the effects of the ionosphere (slant total electron content 10^{17} e cm^{-2}). At high frequencies ($\geq$ 2 GHz) the effects of the ionosphere are negligible and the pulse duation is of order 1 ns. There are now laboratory measurements of coherent Cherenkov and transition radiation from electron bunches in electron linear accelerators (Ohkuma et al 1991; Shibata et al 1991; Takahashi et al 1994). These experiments confirm the quadratic dependence of output power on electron number, and also verify a number of important predictions relevant to the emission process, such as: formation zone effects, finite track–length effects, and interference behavior related to the coherence of the emitted waves. Thus we can begin to have some confidence that predictions of lunar cascade emission should be taken seriously.

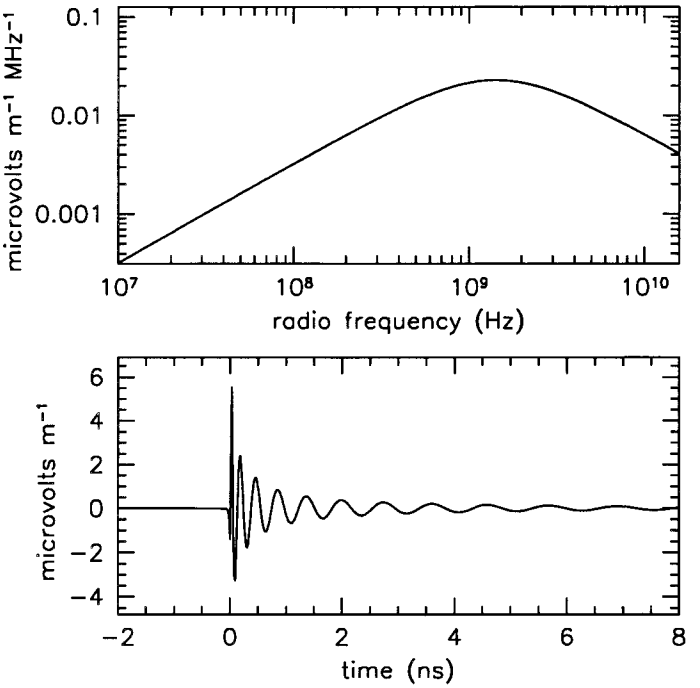

Figure 1: Expected spectrum and shape for a 10^{20} eV lunar cascade radio pulse, including typical ionospheric dispersion.

2 Goldstone Experiment

To investigate the possibility of detecting pulsed lunar cascade emission, we have begun a series of single and dual antenna measurements using the NASA Goldstone Deep Space Station (DSS). The primary antenna is DSS 14, a 70m diameter Cassegrain–design antenna equipped with 1.6-1.7 GHz (L band) single polarization, and 2.2-2.3 GHz (S band) dual polarization receivers, among others. For our dula antenna observations, DSS 14 is paired with DSS 13, a 34 m antenna 21.7 km southeast of DSS 14, connected by a high bandwidth analog optical fiber link. The received electric field is converted to a band-limited voltage at the receiver, then mixed with a local oscillator (LO) to produce an intermediate frequency (IF) of 320 MHz, about which the bandpass of interest appears on the lower sideband.

Our experimental setup for single–antenna measurements involved a trigger system which required a $\geq$ 5 ns coincidence overlap of logic pulses generated directly from the S–band left (LCP) and right (RCP) circular polarization IF bandpass voltages and a fast discriminator. Since Cherenkov emission is 100% linearly polarized, a pulse of Cherenkov radiation will produce an equal amplitude voltage pulse in both LCP and RCP. This type of coincidence is very effective at rejecting interference from microwave telemetry systems (such as those on earth-orbiting satellites) since these are almost universally circularly polarized.

However, such a coincidence is sensitive to impulsive interference, such as that generated by any short-path high-voltage arcing phenomena, which are also typically linearly polarized. Thus a more effective trigger was developed which utilized a second receiver and the L-band feed horn. When DSS 14 is used at S-band, The L-band feed views a region of the sky about 0.5° away, with $\leq$ 0.5% response to an astronomical source (such as the Moon) that is viewed on–axis with the S-band system. Local terrestrial impulsive interference couples to the feed horns either by "flashing" across the sky, or scattering directly from antenna structure (such as the subreflector). Such interference also tends to be steep-spectrum, falling off quickly at higher frequencies.

We found in practice that, by using the L-band signal as a veto, we could virtually eliminate any triggers

from terrestrial interference. This was tested several times at DSS 14, including once under extreme conditions when the trigger rate (for $> 4.5\sigma$ pulses in both polarizations) was 1.5 kHz without the veto. With the veto turned on, the rate of interference triggers decreased to ≤ 0.01 Hz, a factor of $\geq 10^5$ rejection. Such conditions are atypical (average rates of interference triggers are one every few minutes or less), but demonstrate clearly the effectiveness of this method.

Once a trigger is generated, the IF voltage time series for each of the signals present: S-band LCP, S-band RCP, and L-band LCP (veto), are sampled at 1 GHz using a Tektronix TDS784 digital oscilloscope, then read out to computer. Post–analysis of the recorded triggers requires that they are: (1) band-limited in width, consistent with expectations that the cascade pulses are $\sim$ 1ns in duration; (2) not significantly offset in time, or greatly different in amplitude in RCP and LCP; (3) without any significant counterpart in the L-band recorded signal, indicating that they are not likely to be terrestrial in origin; (4) Of sufficient amplitude in each polarization that they are statistically very unlikely from random thermal noise fluctuations.

In the case of the dual antenna system, an additional criterion is included with those above: (5) A band-limited pulse must appear in the DSS 13 IF data coincident in the time window that is consistent with the geometric delay to the surface of the Moon viewed by the two antennas. In practice the width of this window must be of order $B\Theta_m c^{-1} \approx \pm 290$ns (where B is the baseline and Θ_m is the angular size of the Moon) to account for cascades at any point on the Moon's surface.

3 Results

Our hardware trigger was as loose as the data collection system could tolerate, giving trigger rates of 0.1 Hz for the single– and 0.01 Hz for the dual–antenna operation. Since the great majority of these triggers were random thermal noise coincident pulses of the two polarizations our post-processing of the data involved setting a threshold which was well beyond any possibility of random noise coincidence. Thus we required the signals from the 70m antenna (DSS 14) to exceed the 6σ level in both LCP and RCP, along with an additional requirement of $\geq 4\sigma$ from the DSS 13 signal. These requirements can be transformed into an energy threshold for the system, based on the cascade simulations noted above and the standard equation for radio antenna sensitivity: $\Delta S = 2kT_{sys}A_{eff}^{-1}(\Delta t \Delta \nu)^{-0.5}$ W m^{-2} Hz^{-1}. The 1σ thermal noise level for our system is $\sim$ 400 Jy, giving a post-analysis 6σ threshold of 2400 Jy. This in turn corresponds to the flux density expected from a $\sim 1 \times 10^{19}$ eV cascade. Given that virtually all cascades at these energies are expected to be primarily hadronic in nature, the mean of the Bjorken y-distribution implies a mean neutrino energy of a factor of 5 greater than this. Thus we estimate our neutrino energy threshold to be 5×10^{19}eV, with the peak sensitivity (weighted by effective volume and an E^{-2} spectrum) at an energy about a factor of 4–6 higher than this.

We observed the Moon for 4.8 hr on the Moon center, 5.6 hrs at the midpoint from center to limb, and 1.5 hrs at the limb, for a total of 11.9 hrs. Of the $\sim$ 300 dual antenna and $\sim$ 1100 single antenna triggers, none matched all of the criteria above. In both the single– and dual–antenna case, the vast majority of the triggers were simple thermal noise coincidences near the hardware threshold of 4.5σ in each polarization. The remaining triggers are obvious RF interference where the veto pulse level fell below the more conservative ($\geq 5\sigma$) veto threshold, but it still clearly present in the sampled L-band IF data.

3.1 Limits on EHE neutrinos. Figure 2 plots the predicted fluxes of EHE neutrinos from a number of models including AGN production (Mannheim 1996,M) gamma-ray bursts (Waxman & Bahcall 1998,WB), EHE cosmic-ray interactions (Hill & Schramm 1985, HS), and topological defects (TDs; Yoshida et al 1997, YTD; Bhattacharjee et al 1992, BTD; Sigl et al 1996, STD). Also plotted are limits from about 40 days of Fly's Eye livetime (Baltrusaitas et al 1985, FE). Our initial 90% confidence level limit is shown plotted with close-spaced inverted triangles, with the tightest limit at about 10^{20} eV as expected. The behaviour of our differential limit was determined by semi–analytic modelling of the effects of the antenna beam response and the emission geometry and RF attenuation of the regolith.

Our limit conflicts with fluxes predicted in the TD models of Yoshida et al (1997) and Bhattacharjee et al (1992) for which we expected a total of 15 events and 7 events respectively. Also plotted in Fig. 2 are projected limits for the Auger project (Capelle et al 1998) for 5 years of livetime. We include a projection for comparable radio limits using 40 days of livetime, similar to that represented in the Fly's Eye limit. Although this level of livetime may take several years to accumulate, the limit should test almost all of the present models. Fig. 2 also shows the EHE cosmic ray (EHECR) spectrum plotted along with the neutrino predictions and limits. Alvarez–Muñiz & Zas (1996) estimated that the EHECR would dominate the event rates for EHE lunar radio searches. For their predicted fluxes we should have seen 3–4 EHECR–induced events in our data, but saw none. However, we conclude that this prediction is likely to be a significant overestimate in any case, for a number of reasons not considered by Alvarez–Muñiz & Zas: (1) The geometry of EHECR emission causes total internal reflection into the regolith and suppresses emission from downgoing cascades into the regolith to first order; (2) Formation zone effects (cf. Takahashi et al 1994) suppress emission from EHECR cascades that "skim" the regolith surface. We conclude that only narrow ridglines or similar topographic features will be efficient emitters of EHECR radio emission, and the expected rates are far below our limit.

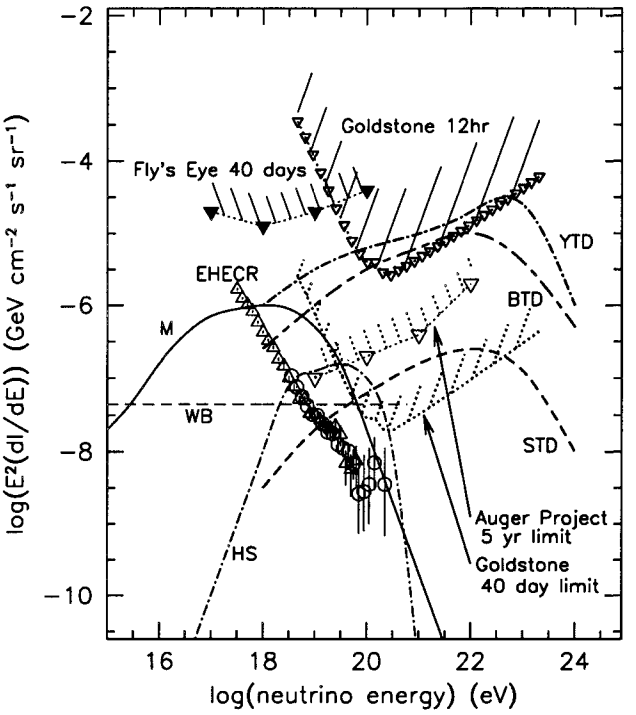

Figure 2: Predictions & limits for EHE neutrinos (details in text).

References

Alvarez–Muñiz, J., & Zas, E., 1997, Phys. Lett. B, 411, 218; also 1998, LANL preprint astro-ph 9806098.

Alvarez–Muñiz, J., & Zas, E., 1996, Proc. XXVth ICRC, ed. M.S. Potgeiter, et al. vol. 7, 309.

Askaryan, G.A.,1962, JETP 14, 441; also 1965, JETP 21, 658.

Baltrusaitas, R.M., Cassiday, G.L., Elbert, J.W., et al 1985, Phys Rev D 31, 2192.

Bhattacharjee, P., Hill, C.T., & Schramm, D.N, PRL 69, 567.

Capelle, K.S., Cronin, J.W., Parente, G., & Zas, E., 1998, Astropart. Phys. 8, 321.

Dagkesamanskii, R.D., & Zheleznyk, I.M., JETP 50, 233.

Hankins, T.H., Ekers, R.D. & O'Sullivan, J.D. 1996, MNRAS 283, 1027.

Hill, C.T., & Schramm, D.N., 1985, Phys Rev D 31, 564.

Mannheim, K., 1996, Astropart. Phys 3, 295.

Ohkuma, J., Okuda, S., & Tsumori, K., 1991, PRL 66, 1967.

Shibata, Y. , Ishi, K., Takahashi, T, et al, 1991, Phys Rev A 44, 3449.

Takahashi, T, Kanai, T., Shibata, Y., et al, 1994, Phys Rev E 50, 4041.

Yoshida, S., Dai, H., Jui, C.C.H., & Sommers, P., ApJ 479, 547.

Zas, E., Halzen, F., & Stanev, T., Phys., 1992, Phys Rev D 45, 362.